

## THE DETAILED OPTICAL LIGHT CURVE OF GRB 030329

Y. M. LIPKIN,<sup>1,\*</sup> E. O. OFEK,<sup>1,\*</sup> A. GAL-YAM,<sup>1,\*</sup> E. M. LEIBOWITZ,<sup>1</sup> D. POZNANSKI,<sup>1</sup> S. KASPI,<sup>1</sup> D. POLISHOOK,<sup>1</sup> S. R. KULKARNI,<sup>2</sup> D. W. FOX,<sup>2</sup> E. BERGER,<sup>2</sup> N. MIRABAL,<sup>3</sup> J. HALPERN,<sup>3</sup> M. BUREAU,<sup>3</sup> K. FATHI,<sup>4,5</sup> P. A. PRICE,<sup>6</sup> B. A. PETERSON,<sup>6</sup> A. FREBEL,<sup>6</sup> B. SCHMIDT,<sup>6</sup> J. A. OROSZ,<sup>7</sup> J. B. FITZGERALD,<sup>7</sup> J. S. BLOOM,<sup>8</sup> P. G. VAN DOKKUM,<sup>9</sup> C. D. BAILYN,<sup>9</sup> M. M. BUXTON,<sup>9</sup> AND M. BARSONY<sup>10,11</sup>

*Received 2003 Dec 7; Accepted 2003 Jan 16*

### ABSTRACT

We present densely sampled *BVRI* light curves of the optical transient associated with the gamma-ray burst GRB 030329, the result of a coordinated observing campaign conducted at five observatories. Augmented with published observations of this GRB, the compiled optical dataset contains 2687 photometric measurements, obtained between 78 minutes and 79 days after the burst. This dataset allows us to follow the photometric evolution of the transient with unprecedented detail. We use the data to constrain the light curve of the underlying supernova 2003dh, and show that it evolved faster than, and was probably somewhat fainter than the type Ic SN 1998bw, associated with GRB 980425. We find that our data can be described by a broken power-law decay perturbed by a complex variable component. The early- and late-time decay slopes are determined to be  $\alpha_1 \approx 1.1$  and  $\alpha_2 \approx 2$ . Assuming this single-break power-law model, we constrain the break to lie between  $\sim 3$  and  $\sim 8$  days after the burst. This simple, singly-broken power-law model, derived only from the analysis of our optical observations, may also account for available multi-band data, provided that the break happened  $\sim 8$  days after the burst. The more complex double-jet model of Berger et al. provides a comparable fit to the optical, X-ray, mm and radio observations of this event. The unique early coverage available for this event allows us to trace the color evolution of the afterglow during the first hours after the burst. We detect a significant change in optical colors during the first day. Our color analysis is consistent with a cooling break frequency sweeping through the optical band during the first day. The light curves of GRB 030329 reveal a rich array of variations, superposed over the mean power-law decay. We find that the early variations ( $\lesssim 8$  days after the burst) are asymmetric, with a steep rise followed by a relatively slower (by a factor of about two) decline. The variations maintain a similar time scale during the first four days, and then get significantly longer. The structure of these variations is similar to those previously detected in the afterglows of several GRBs.

*Subject headings:* Gamma Rays: Bursts — Stars: Supernovae: General — Stars: Supernovae: Individual: Alphanumeric: SN 2003dh

### 1. INTRODUCTION

Following the discovery of low-energy transients associated with long duration ( $> 2$  s) gamma-ray bursts (GRBs; van Paradijs et al. 1997), a major effort was made to characterize the temporal evolution of these sources across the electromag-

<sup>1</sup> School of Physics and Astronomy and the Wise Observatory, Tel-Aviv University, Tel-Aviv 69978, Israel. Electronic address: (yiftah, eran, avishay)@wise.tau.ac.il

<sup>2</sup> Division of Physics, Mathematics and Astronomy, 105-24, California Institute of Technology, Pasadena, CA 91125, USA

<sup>3</sup> Columbia Astrophysics Laboratory, Columbia University, 550 West 120th Street, New York, NY 10027, USA

<sup>4</sup> School of Physics and Astronomy, University of Nottingham, Nottingham, NG7 2RD, UK

<sup>5</sup> Kapteyn Astronomical Institute, P.O. Box 800, 9700 AV Groningen, The Netherlands

<sup>6</sup> Research School of Astronomy and Astrophysics, The Australian National University, Mt. Stromlo Observatory, Weston Creek, P.O., A.C.T. 2611, Australia

<sup>7</sup> Department of Astronomy, San Diego State University, 5500 Campanile Drive, San Diego, CA 92182, USA

<sup>8</sup> Harvard Society of Fellows, 78 Mount Auburn Street, Cambridge, MA 02138.; Harvard-Smithsonian Center for Astrophysics, MC 20, 60 Garden Street, Cambridge, MA 02138, USA

<sup>9</sup> Department of Astronomy, Yale University, New Haven, CT 06520-8101, USA

<sup>10</sup> Department of Physics and Astronomy, San Francisco State University, 1600 Holloway Avenue, San Francisco, CA 94132-4163, USA

<sup>11</sup> Space Science Institute, 3100 Marine Street, Suite A353, Boulder, CO 80303-1058, USA

\* The first three authors contributed equally to this work.

netic spectrum. In the optical regime, the associated transient sources were found to decline rapidly with time. The emission from the first optical transients (OTs) discovered was reported to decay as a power-law with time, extending from the epoch of discovery and continuing for tens of days (e.g., GRB 970228 – Galama et al. 1997; GRB 970508 – Galama et al. 1998a; Sokolov et al. 1998; Bloom et al. 1998).

The decay slopes measured for OTs were used to constrain explosion models. In particular, with the increasing popularity of non-isotropic models (involving highly relativistic jets or cones), a temporal break in the decline slope was predicted (e.g., Rhoads 1997; Panaitescu, Mészáros, & Rees 1998; Sari, Piran & Halpern 1999) – and detected (e.g., Castro-Tirado et al. 1999; Kulkarni et al. 1999; Stanek et al. 1999; Harrison et al. 1999; Price et al. 2001).

Following the discovery of supernova (SN) 1998bw in the error box of GRB 980425 (Galama et al. 1998b) the association of GRBs with SN explosions came into focus. Late-time “bumps” in OT light curves were interpreted as the signature of underlying SN explosions (e.g., Bloom et al. 1999). While observational evidence supporting the SN hypothesis accumulated (e.g., Bloom et al. 2002; Garnavich et al. 2003; Price et. al. 2003a), a direct observational proof for the existence of an underlying SN explosion has long remained missing, and alternative explanations for the origin of these bumps were suggested (e.g., Waxman & Draine 2000; Esin & Blandford 2000; Reichart 2001).

With growing interest and efforts by the astronomical com-

munity, the observed OT light curves became increasingly better-measured. In particular, for some OTs, a dense temporal sampling of the light curve, sometimes starting shortly (minutes to hours) after the GRB trigger, was carried out by world-wide observing networks. A case to point is the OT of GRB 021004, where multiple bumps and wiggles in the light curve, probably not associated with a SN, were first observed (e.g., Bersier et al. 2003; Mirabal et al. 2003; Fox et al. 2003).

On 2003 March 29, a bright GRB was detected by the HETE-II spacecraft (Vanderspek et al. 2003). The early discovery of the associated OT (Peterson & Price 2003; Torii 2003; Torii et al. 2003; Price et al. 2003b; Uemura et al. 2003; Sato et al. 2003), and its brightness, triggered a world-wide observational effort, involving tens of ground and space-based facilities, observing in various wavelengths, from X-ray to radio. The brightness of the OT allowed the prompt determination of the redshift of the source. At  $z=0.1685$  (Greiner et al. 2003a) this event is the closest GRB to date for which a typical OT was discovered. The relatively low redshift of this burst presented a unique opportunity to search for a clear spectroscopic signature of an underlying SN. Indeed, intensive spectroscopic monitoring of the optical source revealed the emerging spectrum of a type Ic SN 1998bw-like event, designated SN 2003dh, conclusively proving that at least some of the long-duration GRBs are associated with SN explosions (Stanek et al. 2003; Hjorth et al. 2003; Matheson et al. 2003).

Numerous works have already presented observations of this unique event. Early optical observations, obtained with small telescopes shortly after the burst, were reported by Uemura et al. (2003), Torii et al. (2003), Smith et al. (2003), Sato et al. (2003), and Urata et al. (2003). Burenin et al. (2003), Bloom et al. (2003) and Matheson et al. (2003) presented the results of multi-band follow-up campaigns in the optical and near-IR. Greiner et al. (2003b) presented optical polarization monitoring of GRB 030329, detecting significant variability. These works mostly relied on data collected at a single geographical location, thus limiting their ability to achieve a continuous temporal coverage. Intensive monitoring of the afterglow of GRB 030329 in the radio and millimeter wavelengths was reported by Berger et al. (2003) and Sheth et al. (2003), while X-ray observations were reported by Tiengo et al. (2003).

In this paper, we report the results of an intensive, coordinated, world-wide campaign designed to follow the light curve of the OT associated with GRB 030329. Combining data from five observatories in three continents, we achieved an almost continuous coverage of the OT during the first few days after the GRB. Careful cross-calibration was used to bring data collected using many different instruments to the same reference system. This internally-consistent data set has allowed us to correctly incorporate four other sets of observations now available in the literature. The final light curves which we compiled are unprecedented in their temporal sampling, and reveal a uniquely rich and complicated photometric evolution. We assume throughout a cosmology with  $\Omega_m = 0.3$ ,  $\Omega_\Lambda = 0.7$ ,  $H_0 = 65 \text{ km s}^{-1} \text{ Mpc}^{-1}$ .

## 2. OBSERVATIONS AND DATA REDUCTION

We performed time-resolved CCD photometry of the OT at five observatories, from March 29.72 to June 17.19 UT (5.66 hr. to 79.7 d after the burst). Observations were carried out through  $B$ ,  $V$ ,  $R$ , and  $I$  filters, accumulating a total of 77, 104, 928, and 96 data points, respectively. Details of

TABLE 1. LIST OF OBSERVATORIES

ID	Observatory+Instrument	E. long.	Filter (number of observations)
01	Wise 1m+Tek	34.8	B(9), V(25), R(484), I(25)
02	Wise 1m+SITe	34.8	B(8), V(7), R(57)
03	SSO 1m+WFH	149.1	B(5), V(2), R(5), I(2)
05	MDM 1.3m+2.4m+SITe	-111.6	B(1), V(1), R(311), I(1)
06	Palomar 1.5m+Norris	-116.9	I(3)
07	Mt. Laguna 1m+Loral	-116.4	B(54), V(69), R(71), I(67)
21	Kyoto <sup>a</sup>	~135	CR(391) <sup>e</sup>
31	RTT <sup>b</sup>	30.3	B(144), V(167), R(168), I(165)
41	CTIO 1.3 <sup>c</sup>	-70.8	B(9), V(13), I(13)
51	FLWO <sup>d</sup>	-110.9	B(62), V(57), R(111), I(57)
52	KAIT <sup>d</sup>	-121.6	B(14), V(15), R(15), I(15)
53	LCO <sup>d</sup>	-70.7	B(4), V(4), I(4)
54	LCO-40 <sup>d</sup>	-70.7	R(2)
55	KPNO4m <sup>d</sup>	-111.6	B(19), R(4)
56	Magellan2 <sup>d</sup>	-70.7	R(25)
57	Dupont <sup>d</sup>	-70.7	B(4)

NOTE. — The upper part of the table lists the observatories which took part in our campaign. The lower part lists external data sources.

<sup>a</sup>Several observatories in Japan. Uemura et al. (2003).

<sup>b</sup>Burenin et al. (2003).

<sup>c</sup>Bloom et al. (2003).

<sup>d</sup>Matheson et al. (2003).

<sup>e</sup>Unfiltered observations transformed to  $R$ -band, see Uemura et al. (2003).

TABLE 2. REFERENCE STARS

Coordinates (2000)	Number <sup>a</sup>	V mag <sup>a</sup>	Used in sets <sup>b</sup>
10:44:28.62 +21:27:45.4	005	15.587	2 3 6
10:44:36.86 +21:26:59.1	016	13.266	6
10:44:39.07 +21:30:59.1	019	17.616	1 3 6 7
10:44:39.86 +21:34:15.0	021	16.842	1 3 6
10:44:41.75 +21:31:52.6	026	19.331	3 5 7
10:44:42.02 +21:32:32.1	027	16.839	2 3 5 7
10:44:48.03 +21:34:18.5	037	17.909	1 2 3
10:44:53.66 +21:30:12.1	047	18.396	6
10:44:54.45 +21:34:29.2	049	14.136	3
10:44:54.99 +21:29:46.3		20.275 <sup>c</sup>	5
10:44:55.00 +21:31:42.9	050	19.598	7
10:45:06.48 +21:36:13.7	093	16.245	2
10:45:09.81 +21:35:10.2	098	15.469	2 3
10:45:15.36 +21:34:16.1	110	14.730	2 3 6

<sup>a</sup>Star numbers and magnitudes refer to the photometry of Henden (2003).

<sup>b</sup>Observatory IDs given in Table 1.

<sup>c</sup>Photometry measured in our dataset, and scaled to the system of Henden (2003)

the equipment and a summary of the observations are given in Table 1.

The images were bias-subtracted and flat-field corrected in the standard fashion. In each frame we measured the magnitude of the OT, as well as of several reference stars, with an aperture of 2 arcsec radius. Three to nine reference stars were measured in each subset, depending on the depth and the field of view of the images. All of the reference stars were tested to be non-variable. The reference stars used in each subset are listed in Table 2.

For each of the detectors used, we obtained a set of internally-consistent magnitudes of the OT by minimizing the scatter of the reference stars over the subset. Outlying measurements were removed during the process. Apparently underestimated errors in the photometry of reference stars were

increased so that  $\chi^2/dof = 1$  (where *dof* is the number of degrees of freedom) for each of the reference stars in the subset.

Cross calibration, including color terms, of the different instruments was carried out by transforming the photometric system of each of the subsets to the one of Henden (2003). The transformation parameters were derived by linearly fitting the differences between the weighted-mean magnitude of the reference stars, and their magnitudes in the Henden (2003) system, to the colors of the reference stars reported by this author. Because of the initial uncertainty in the OT colors, two iterations were required to transform its magnitude to the reference system. The transformation uncertainty of each data subset was added in quadrature to the measured photometric errors. The photometric errors do not include the uncertainty in the zero point of the calibration, 0.02 mag (Henden 2003).

The photometric measurements obtained at the Mount Laguna Observatory failed to yield consistent color terms and were therefore cross-calibrated by eliminating the offset between overlapping segments of this subset and the rest of the light curve. From the residual scatter in these overlapping segments, we estimate the resultant systematic cross-calibration errors of this set to be  $\sim 5\%$ .

We augmented our data set with external photometry from Burenin et al. (2003), Uemura et al. (2003), and Bloom et al. (2003), kindly provided in digital form by the authors, as well as with the data published by Matheson et al. (2003). Each of the external data sources was cross-calibrated with our set using the procedure described above for the Mount Laguna Observatory data. Since the color of the OT changed with time, this process may have introduced small systematic errors. From the scatter between the external sets and our light curves, we estimate this error to be smaller than 5%.

A few data segments from Uemura et al. (2003), temporally overlapping with our own, were not incorporated into our light curve because the photometric errors in these segments (and hence the scatter of the data points) were greater than in our data. We note, however, that our data and those of Uemura et al. are in good agreement throughout the overlapping segments. The *I*-band light curve of Burenin et al. (2003), covering the time-span between 0.2 d and 0.6 d, does not overlap with our *I*-band data. The zero point for this segment was set by coarsely extrapolating later *I*-band segments, and should therefore be regarded with caution.

The earliest available observations of the OT ( $\sim 1.3$  hr after the burst) were obtained by two groups. A set of unfiltered observations were reported by Uemura et al. (2003), who transformed the resulting magnitudes to the standard *R*-band. After cross calibration, these data are in good agreement with the rest of our data. A couple of measurements in standard *R* were taken through clouds with the SSO 1m telescope (Price et al. 2003b). After cross-calibration, the two points yielded significantly brighter measurements, by about 0.1 mag. Other observations from the SSO 1m telescope, taken under better conditions, are in good agreement with the rest of the data. Because of the good agreement between the bulk of our data and those of Uemura et al. (2003), and because of the unfavorable weather conditions under which the early SSO images were obtained, we preferred the light curve of the former over the latter two points. The results we present below, however, are insensitive to this selection, and would remain essentially the same had we corrected Uemura's data to fit the SSO points. The recently reported early observations by Torii et al. (2003) are even brighter than the SSO points. Thus,

TABLE 3. OBSERVATIONS

(1)	(2)	(3)	(4)	(5)	(6)	(7)
01	04	2729.21443	1.23024	16.438	0.018	0.050
01	04	2729.21597	1.23177	16.414	0.020	0.051
01	04	2729.21749	1.23329	16.447	0.018	0.050
01	04	2729.21900	1.23481	16.398	0.019	0.050
01	04	2729.22052	1.23632	16.415	0.018	0.050
01	04	2729.22203	1.23783	16.432	0.018	0.050
01	04	2729.22355	1.23936	16.434	0.018	0.050
01	03	2729.22956	1.24536	16.786	0.012	0.022
01	05	2729.23286	1.24866	15.940	0.011	0.060
01	04	2729.23549	1.25129	16.416	0.013	0.048

NOTE. — The first ten data points of our light curve. The columns are: (1) the observatory code (see Table 1); (2) the filter used. 2,3,4,5 are for *B*, *V*, *R*, *I*, respectively; (3)  $JD - 2450000$ ; (4) time since  $t_{burst} = 2452727.98419757$ ; (5) calibrated magnitude; (6) the error in magnitude including the self calibration error of the individual observatory; (7) the error in magnitude including the uncertainty in cross calibrating the various observatories.

it appears that forming a consistent picture of the early light curve of this event will require further analysis, once all the relevant data are available.

Altogether, we compiled 2687 photometric measurements (333, 360, 1644, and 350 in *B*, *V*, *R*, and *I*, respectively), making GRB 030329 the most extensively studied extragalactic cosmic explosion in the optical regime, with the possible exception of SN 1987A. The complete set of photometric measurements presented in this paper are listed in Table 3<sup>13</sup>.

### 3. THE LIGHT CURVE

The final *BVRI* light curves of GRB 030329 are presented in Figure 1. Our best-sampled set is the *R*-band light curve, with an almost continuous coverage during  $0.05 \lesssim t \lesssim 3$  d, and a relatively dense sampling up to  $t \approx 67$  d. We therefore focus our attention on this light curve, and, augment our analysis with results from other bands when necessary.

While the OT grossly follows a power-law declining trend, it shows remarkably strong short-term deviations from the smooth, monotonic decline, particularly between  $0.05 \lesssim t \lesssim 5$  d. Later periods, between  $8 \lesssim t \lesssim 14$  d, and at  $t \gtrsim 50$ , also feature pronounced variations of the light curve. We note that the light curves do not show *a priori* any clear distinction between “early” and “late” power law components – the signature of a break in the decline rate. We also note the lack of a clear bump which may be attributed to SN 2003dh, although its significant contribution to the total brightness of the OT was established spectroscopically.

At  $R = 23.25 \pm 0.15$  mag (Fruchter 2003, Priv. Comm.), the host becomes a significant contributor to the observed flux during the late decline phase of the OT. Hence below, unless stated otherwise, we shall discuss the R-band light curve of the OT only, obtained by subtracting the host flux from our measurements. The photometric errors of the OT were modified to include the uncertainty in the host galaxy magnitude.

To further discuss the light curve, we decompose it into a SN component, and an “afterglow” component, which is further divided into two components: a smooth, monotonic decline component (the main observational characteristic of GRB afterglows), and a perturbations component – variations

<sup>13</sup> The complete Table with all 2687 measurements is given in the electronic version of this paper. The data are also available from our web site: <http://wise-obs.tau.ac.il/GRB030329/>

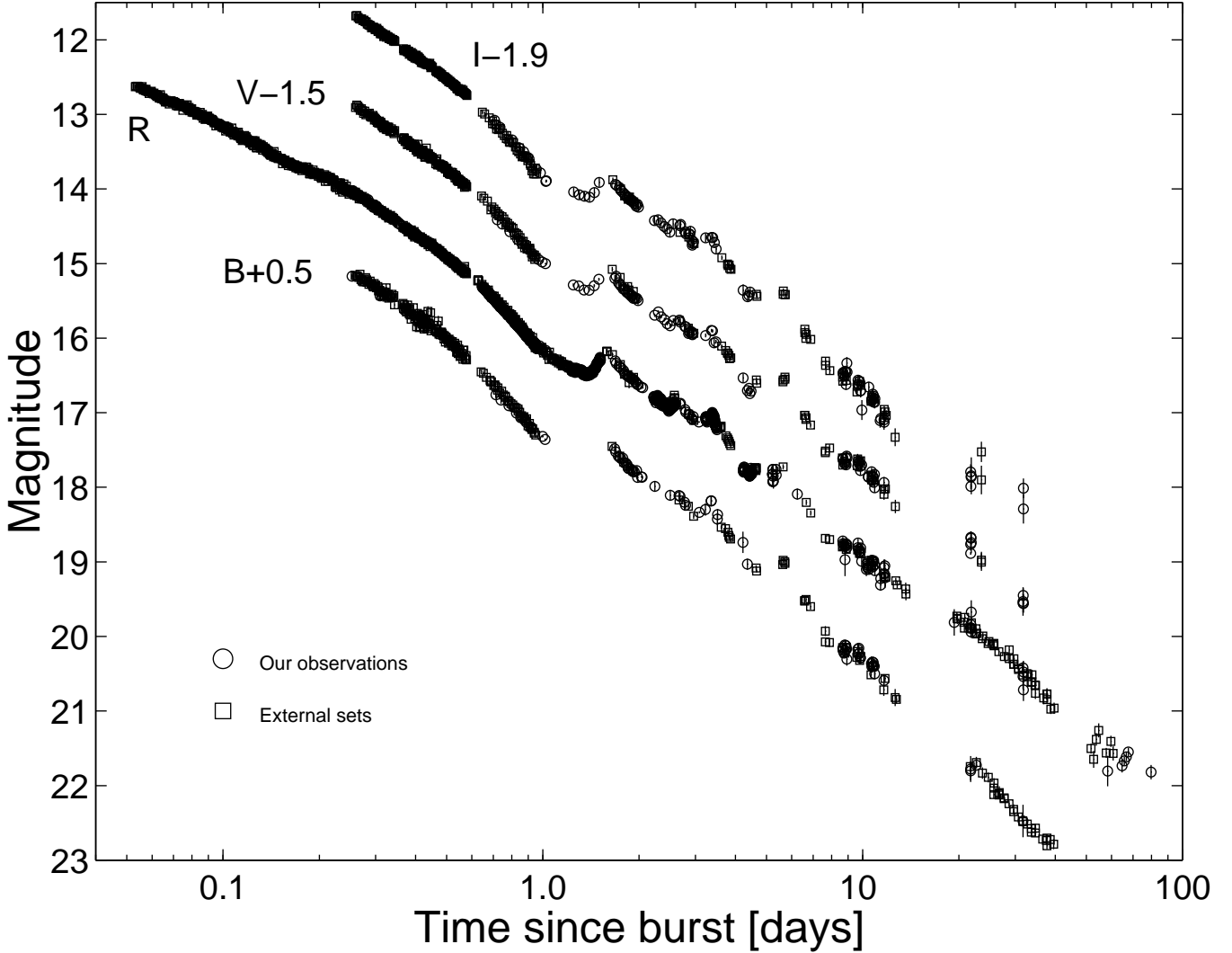


FIG. 1.— *BVRI* light curve of GRB 030329. Our observations are marked by circles, and the external data sets (see Table 1), cross-calibrated to our photometric system, are marked by squares. For presentation purposes the *BVI* light curves are shifted vertically by +0.5, -1.5, and -1.9 mag, respectively.

over different time scales and intensities about the smooth decay of GRB 030329. In the following sections we shall consider each of the OT components separately.

### 3.1. The supernova component

Spectroscopic analysis of SN 2003dh (Stanek et al. 2003; Hjorth et al. 2003; Matheson et al. 2003; Chornock et al. 2003) revealed a remarkable similarity to the well studied SN 1998bw associated with GRB 980425 (although, see Mazzali et al. 2003; Kawabata et al. 2003). In light of this similarity, we base our investigation of the SN component in the afterglow of GRB 030329 on the known properties of SN 1998bw.

We constrain the SN component by comparing the OT light curve with four alternative models for SN 2003dh. All four models are modifications of the light curve of SN 1998bw, corrected to the redshift of SN 2003dh ( $z=0.1685$ ). The transformation was carried out by applying synthetic photometry (using the methods presented in Poznanski et al. 2002) to the large collection of SN 1998bw spectra reported by Patat et al. (2001), and taking into account the greater luminosity distance of SN 2003dh (810 Mpc, compared to 37 Mpc

of SN 1998bw), cosmological redshift and time-dilation effects, as well as the shift in the SN spectrum sampled by each filter (K-corrections). The SN light curve was also corrected for Galactic extinction in the direction of SN 2003dh ( $E_{B-V} = 0.025$  mag, Schlegel, Finkbeiner, & Davis 1998), but was not corrected for the host galaxy extinction (see below). Our derived light curves are in good agreement with those computed by Bloom et al. (2003) using a slightly different approach.

Comparing the models to the data, we note that any variation in the light curve should probably be attributed to the afterglow, since no such variations have been detected in the light curves of any of the well observed SNe Ic (e.g., SN 1998bw – Galama et al. 1998b; McKenzie & Schaefer 1999; Patat et al. 2001; SN 2002ap – Gal-Yam, Ofek & Shemmer 2002; Panday et al. 2003; Yoshii et al. 2003; Foley et al. 2003; SN 1999ex – Stritzinger et al. 2002; SN 1994I – Yokoo et al. 1994). A valid SN model is therefore required to be fainter than the bottom of the dips in the light curve. In particular, the minima of two rebrightening episodes in the *R*-band, one of  $\sim 0.3$  mag around  $t \approx 52$  d, and another of  $\sim 0.2$  mag

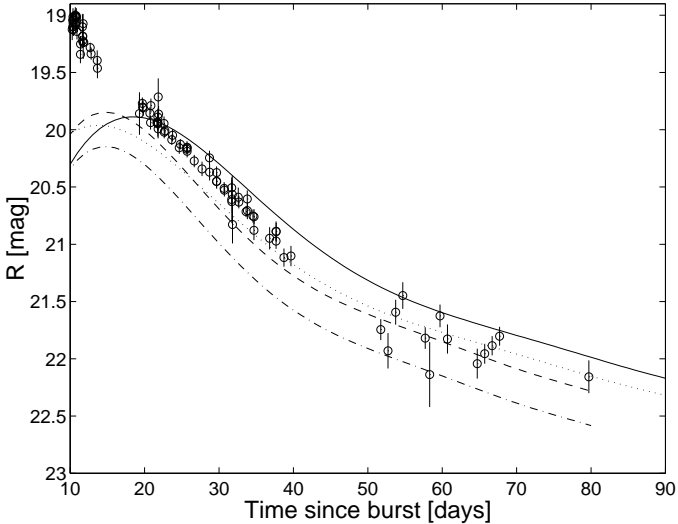


FIG. 2.— The host-subtracted  $R$ -band light curve of the OT (open circles) compared to four model light curves of SN 2003dh. The plotted lines are: the light curve of SN 1998bw, redshifted and K-corrected (solid line); the same model, after applying the best fitting magnitude shift and temporal shift relative to the GRB (see text; dotted line); the same model, after applying the best fitting magnitude-shift and stretch correction (see text; dashed line); and the time-stretched and magnitude-shifted model lowered by 0.3 mag (dash-dotted line).

around  $t \approx 68$  d (see §3.3) set upper limits on the SN magnitude of  $R = 21.93 \pm 0.15$  and  $R = 22.04 \pm 0.13$  mag at the times of these episodes, respectively.

Figure 2 shows the  $R$ -band light curve of the OT (open circles). Overlaid are the four different model light curves for the supernova component. The solid line in Fig. 2 is the redshift-corrected light curve of SN 1998bw described above, assuming it exploded simultaneously with the GRB. This simple model is consistently brighter than the data points after day  $\sim 20$ , and is therefore ruled out – had SN 2003dh been identical to SN 1998bw, the OT would have been brighter than observed after day 20.

Hjorth et al. (2003) decomposed their observed spectra into a SN Ic component (using redshifted versions of SN 1998bw spectra) and a power-law component, typical for the optical emission from cosmological GRBs. Using this method, these authors derived a  $V$ -band light curve of the SN component during the first month after the GRB. They found that their data could not be fitted by a redshifted and K-corrected  $V$ -band light curve of SN 1998bw (see their Fig. 3), but required that the SN component would be slightly brighter (by  $\sim 0.2$  mag) at the peak, and would also decline much faster than SN 1998bw, becoming at least 0.7 mag fainter 28 days after the GRB. Similar results were obtained by Mazzali et al. (2003), who combined spectral analysis with explosion models.

With this in mind, we consider alternative models for the SN component. Following Hjorth et al. (2003) and motivated by theoretical models of delayed core-collapse (e.g., Vietri & Stella 1998; Berezhiani et al. 2003), we consider a non-simultaneous SN model. The model light curve (dotted line) was obtained by fitting the  $V$ -band light curve of SN 1998bw to that of SN 2003dh (Hjorth et al. 2003), with two free parameters: a time lag between the GRB and the SN explosion ( $\Delta T$ ), and a magnitude-correction ( $\Delta m$ ). The best fit values are:  $\Delta T = -4.7^{+1.7}_{-2.2}$  d and  $\Delta m = 0.08 \pm 0.10$  mag,

with  $\chi^2/dof = 2.5/4$ . This model initially agrees with the data, but becomes too bright after day 50, and is therefore discarded. Larger temporal offsets (required to make the SN fainter at late times) are inconsistent with the spectral analysis of Stanek et al. (2003), Matheson et al. (2003), and Hjorth et al. (2003). In the next model (the dashed line in Fig. 2), we introduced a magnitude correction parameter ( $\Delta m$ ), and a "stretch" parameter  $s$  (similar to the formalism used by Perlmutter et al. 1999) which adjusts the width of the light curve so that the model luminosity of SN 2003dh at time  $t$  after the burst is given by the luminosity of the redshifted SN 1998bw at  $t/s$ . We find  $s = 0.80 \pm 0.05$  and  $\Delta m = -0.01 \pm 0.10$  (with  $\chi^2/dof = 0.9/4$ ) by fitting the  $V$ -band light curve of SN 1998bw to the measurements of Hjorth et al. (2003). This model provides a somewhat better fit to the data compared to the delayed-GRB model (dotted line), but still overestimates the data after day 50.

In search for a SN model which will satisfy all available constraints, we consider two additional inputs. Bloom et al. (2003) used a self-consistent multicolor data set obtained with a single instrument (ANDICAM, mounted on the CTIO 1.3m telescope). They found that their data could be adequately modeled using the redshifted and K-corrected light curves of a SN 1998bw-like event, which is slightly brighter than SN 1998bw. Such light curves are ruled out by our measurements, obtained from day 20 onward. The probable reason for SN 1998bw being consistent with the observations of Bloom et al. (2003), is that their data are well sampled until day 12, and their latest data points were obtained at day 23, just when our data start indicating that SN 1998bw-like light curves are too bright.

Matheson et al. (2003) did not pursue the full calculation of K-corrections required to produce the light curves of SN 1998bw as they would appear for an event exploding at  $z = 0.1685$ . Instead, they used the  $V$ -band light curve of SN 1998bw as a proxy for the  $R$ -band light curve of SN 2003dh. Comparing their adopted "R-band" light curve with the results of our own calculation, we find that their light curve has a similar shape, but is fainter by  $\sim 0.4$  mag, taking into account their estimated extinction  $A_R < 0.2$  mag. In their SN light curve model, Matheson et al. (2003) further scaled down SN 2003dh by  $\sim 0.2$  mag, relative to their adopted SN 1998bw light curves. Thus, the good fit they reported for SN 1998bw-like light curves is actually for an event fainter by  $\sim 0.6$  mag.

Because our late-time data rule out non-stretched SN 1998bw-like light curves, even if they are as faint as advocated by Matheson et al. (2003), we are led to construct a model, which is identical to the stretched model (dashed-line), but is attenuated by 0.3 mag (the dash-dotted in Fig. 2) – a compromise between the results of Bloom et al. (2003) and Hjorth et al. (2003), suggesting peak magnitudes at least as bright as those of SN 1998bw, and those of Matheson et al. (2003), who found that SN 2003dh was fainter than SN 1998bw by  $\sim 0.6$  mag. This last model seems to best fit both our data and other available studies, and is also in good agreement with the theoretical modeling reported by Mazzali et al. (2003). Both the attenuation factor and the stretch parameter of this last model are well situated in the parameter space of fitted 1998bw-like SN, which was obtained by Zeh, Klose & Hartman (2003) for a sample of seven GRB optical counterparts. Note, that we do not correct for the host-galaxy extinction of SN 2003dh. If we assume negligible extinction of SN 1998bw and the maximal extinction values allowed by the

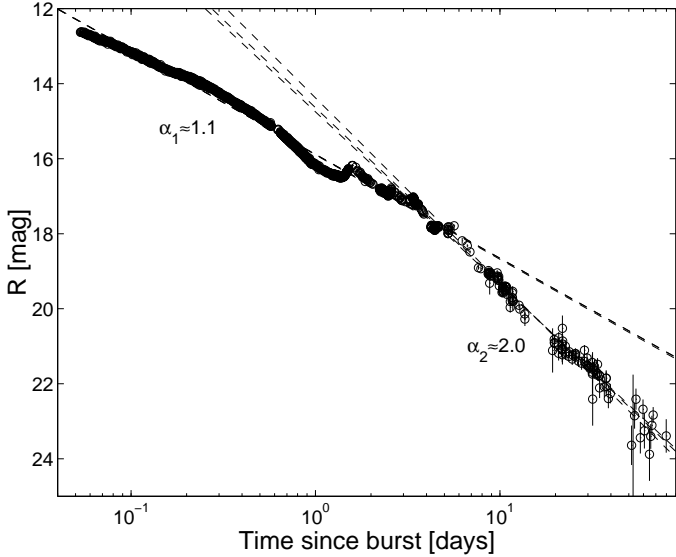


FIG. 3.—  $R$ -band light curve of the afterglow. The light curve was derived by subtracting the contribution of SN 2003dh and of the host galaxy from the observed light curve. Overlaid are a few power-law fits to early and late times (see text for details). A break at  $t \sim 5$  days is apparent. The slope of the pre-break power-law is  $\alpha_1 \approx 1.1$ , and that of the post-break is  $\alpha_2 \approx 2.0$ .

analysis of Matheson et al. (2003) and Bloom et al. (2003),  $A_V \lesssim 0.4$ , our adopted peak magnitude may be consistent with that of a SN which is intrinsically identical to SN 1998bw. The  $\Delta m = 0.3$  magnitude we adopted for the attenuation of SN2003dh relative to SN1998bw, is in fact a lower limit on the attenuation (or conversely, an upper limit on the allowed peak luminosity). Therefore, below we further check the robustness of our results to the value of attenuation we adopt in our SN model.

### 3.2. The afterglow component

The clearcut connection between GRB 030329 and SN 2003dh makes it important to characterize the afterglow in detail, in order to check whether this is a typical burst, or an exceptional one. Figure 3 shows the  $R$ -band light curve of the afterglow, derived by subtracting the host galaxy flux and the preferred SN model (dash-dotted line in Figure 2, see §3.1 for details). The afterglow light curve is clearly not a smooth decline - strong variations are apparent, starting very early after the burst, and continuing throughout our observations (§3.3). Inspection by eye shows that the early light curve may be described by a power-law decline, with a steepening of the slope around  $t \sim 5$  d.

We therefore begin our examination by investigating the simplest plausible model – a singly-broken power law. We fitted sets of double power laws to the afterglow light curve. In each fit, we assumed a different break time  $t_{\text{break}}^{\text{assumed}}$  (i.e., one power law was fitted to all the points with  $t < t_{\text{break}}^{\text{assumed}}$  and another one to points with  $t > t_{\text{break}}^{\text{assumed}}$ ). The intersection time ( $t_x$ ) of the two power-laws, and the sum of the  $\chi^2$  values of the two fits were calculated for each  $t_{\text{break}}^{\text{assumed}}$ . During the first three days, the light curve was sampled more intensively than at later times. To reduce the overwhelming statistical weight of this segment, we diluted it by binning the points. The dashed lines in Fig. 3 are a few examples of such fits, with  $t_{\text{break}}^{\text{assumed}} = 3, 5, 8$  d. As can be seen, the values of the early- and late-time slopes are weakly dependent on the assumed

break time. We therefore consider these values ( $\alpha_1 \approx 1.1$  and  $\alpha_2 \approx 2.0$ , where  $\alpha$  is the power-law decay index defined by the dependence of flux,  $f$ , on time  $f \propto t^{-\alpha}$ ) to be robustly constrained by the data.

For assumed break times between 1.5 and 11 d, the calculated intersection between the two power-law fits fall consistently between 3 and 5 d. Minimum  $\chi^2$  values were obtained for assumed breaks between 3 to 6 d. When carried out with light curves in the  $B$ ,  $V$  and  $I$  bands, the same procedure yielded a similar range for the intersection points:  $3 \lesssim t_x \lesssim 8$  d.

To test the sensitivity of our results to the SN model which was subtracted from the light curve, we repeated the test using several different SN models. All the models were redshift- and K-corrected light curves of SN 1998bw, stretched by  $s = 0.80$ . We varied the values of the attenuation  $\Delta m$  between  $0.3 \leq \Delta m \leq 0.6$  mag, since brighter values ( $\Delta m < 0.3$ ) are ruled out by our light curves (see § 3.1), and fainter values ( $\Delta m > 0.6$ ) are inconsistent with the strength of the observed SN features in the OT spectra (Matheson et al. 2003; Hjorth et al. 2003). The early-time slope did not change significantly, while the late-time slope varied between 1.8 – 2.0, leaving the range of intersection times unchanged.

To conclude, for a singly broken power law model, our data robustly constrain the early- and late-time decay slopes to lie around  $\alpha_1 \approx 1.1$  and  $\alpha_2 \approx 2.0$ , respectively. These values depend very weakly on the light curve segments used, or on the SN model subtracted. If we take the intersection time of these slopes as an estimate for the break time, the resulting values lie around  $t \sim 5$  d. However, because of the strong variations in the light curve, the time of the break is not well constrained, and could be placed at any time between  $\sim 3$  to  $\sim 8$  d. If we adopt  $t_{\text{break}} = 5$  d for the time of the break, a fit to the data before and after the break yields  $\alpha_1 = 1.11 \pm 0.01$  and  $\alpha_2 = 1.96 \pm 0.02$ . Maintaining self-consistency, the intersection of these two power laws is  $t_x = 4.9$  d. This result agrees with the late-time power-law slope,  $\alpha = 2.05$ , measured by Matheson et al. (2003) from data obtained between  $t \approx 5$  d to  $t \approx 61$  d. It appears that a double-power law, broken somewhere between day  $\sim 3$  and  $\sim 8$ , and strongly perturbed by a series of bumps (Figures 3 and 4) provides a fair description of the complex light curve of this OT. We therefore continue and analyze the properties of the variable component derived from the simple broken power-law model in the next section.

Numerous works, analyzing short or sparsely-sampled optical light curves, have interpreted some of the deviations from a smooth decline observed in the OT light curves as manifestations of specific phenomena predicted by popular relativistic jet models. In particular, Berger et al. (2003) propose a model that attempts to consistently account for observations in the radio, mm, optical and X-ray bands. We review the complex structure seen in our superior data in the context of previous analyses in section §4.1 below, and confront an updated version of the Berger et al. (2003) model with our optical observations in §4.2.

### 3.3. The variable component

Subtracting our best double power-law decline model (§3.2) from the afterglow light curve, we derive the residual  $R$ -band light curve of the afterglow. Three segments of the residual light curve are shown in Figures 4, 6 and 7.

Figure 4 shows the residual light curve during the first eight days after the burst. Arbitrarily, we consider the variability as a series of bumps, although with no model at hand, this is a

mere matter of convenience. The bumps in Fig. 4 are marked according to the notation introduced by Granot, Nakar, & Piran (2003), who identified four bumps in the light curve of the OT, compiled from reports in GCN circulars (*A*, *B*, *C*, and *D* in Fig. 4). The early bump,  $\aleph$ , was identified by Uemura et al. (2003), and the minor bumps, *A'* and *C'* are introduced in this work. The validity of the minor bump *C'* is uncertain, because the peak of the bump is only  $\sim 1\sigma$  brighter than the dip prior to the bump, and since the points forming its peak all come from the same data set (Matheson et al 2003).

The bumps before day  $\sim 8$ , which possibly occurred prior to the change in the afterglow decline rate (Fig. 4, see § 4.3 below) are asymmetric in shape, with an incline that is typically  $\sim 2$  times as steep as the decline (with the possible exception of *C'*, which is poorly sampled).

Bumps *A*, *B*, and *C* share a strikingly similar overall structure and time-scale during  $\sim 0.6$  d about their maximum. This similarity is demonstrated in Fig. 5 (panels *a*, *b*, and *c*), where each of the three bumps is shown, compared to a curve manifesting the common coarse structure of these bumps. To derive this “standard profile” of the bumps, we superposed bumps *B* and *C* over bump *A*. Bumps *B* and *C* were shifted by  $\Delta T = -1.02$  d,  $\Delta m = -0.008$  mag, and  $\Delta T = -1.718$  d,  $\Delta m = 0.055$  mag, respectively, to obtain a good match by eye. The data were then smoothed using cubic splines. Finally, we derived a profile curve using a high-degree polynomial fit.<sup>14</sup>

The three events are consistent with this “standard profile”, comprising of a fast monotonic rise, and a slower, complex decline. Panels *d*, *e*, and *f* in Fig. 5 show a comparison between the “standard profile” and bumps  $\aleph$ , *A'*, and *D*, respectively. The brightening rate of bump  $\aleph$ , as well as its time scale, are similar to the standard profile. However, its structure is significantly different. In particular, in contrast to the concave early decline which *A*, *B*, and *C* seem to share, the declining branch of  $\aleph$  has a convex form. Our fragmented data of bump *D* are consistent with the standard profile, but on a time scale that is longer by a factor of  $\sim 2 - 2.5$ . Finally, the rising branch of minor bump *A'* seems to be similar to the tip of standard profile, but its decline is slower, perhaps because of the rising of bump *B*.

Another apparent phase of variability, between 8 d and 13 d, features three consecutive low-amplitude ( $\Delta R \approx 0.1$  mag) bumps, with a time-scale of  $\sim 1$  d (Fig. 6). However, the amplitudes of the later two bumps ( $t \sim 10.7$  and  $t \sim 11.7$  d) are within the cross calibration systematic uncertainties, and their maxima data all come from a single source (Mount Laguna Observatory), and should be therefore treated with caution until confirmed by other observations. A broad bump (*F*) spanning  $\sim 20$  d occurred around  $t \approx 30$  d (Fig. 7). The shape of this feature is somewhat sensitive to the SN model used. Nevertheless, the deviation from the power-law decline during this period persists for any of the SN models which we have tested.

Strong variability is also detectable during the late decline, after  $t \sim 50$  d. In particular, a  $\sim 0.3$  mag rebrightening on a time scale of 2 d occurred around  $t \approx 52$  d (the “jitter episode” of Matheson et al. 2003; See Fig. 3). Our light curve features another  $\sim 0.2$  mag rebrightening on a time scale of a few days, around  $t \approx 64$  d. Because the observations tracing this variation were all obtained at the same observatory (MDM 2.4m), it is unlikely that this is due to some reduction artifact. To con-

clude, it appears that successful models of this well-observed GRB should ultimately account for strong variations of the optical emission, on time scales of hours to weeks, recurring over tens of days after the burst.

### 3.4. Color evolution

Figure 8 shows the  $B - R$  color evolution of the light curve of GRB 030329. The host and the SN light curve were not subtracted, in order to reduce propagated errors and keep the results model-independent. To derive the  $B - R$  light curve we interpolated the better sampled *R*-band light curve onto the times of the *B*-band light curve. The interpolation uncertainty was calculated using the method of Ofek & Maoz (2003). Finally, we binned the  $B - R$  color light curves in 0.05 d bins.

The color evolution of this event was studied in detail by Matheson et al. (2003) and Bloom et al. (2003). Both groups used subsets of the data presented here. Our analysis yields consistent results with those previous works. In particular, we measure almost constant colors between days 2 – 5, after which the emerging SN component (with colors similar to SN 1998bw) drove the color evolution of the optical emission. Furthermore, the earlier coverage of our light curves enables us to measure the color evolution of the OT during the first day.

The  $B - R$  light curve shows a small ( $\sim 0.1$  mag), but significant, color variation during the first day after the burst (Figure 8, inset). The color of the OT evolved from  $B - R = 0.58 \pm 0.01$  mag at  $t = 0.28$  d (corresponding to  $\beta_{BR} = -0.88 \pm 0.02$ ) to  $B - R = 0.66 \pm 0.02$  mag at  $t = 0.83$  d (corresponding to  $\beta_{BR} = -1.07 \pm 0.05$ ), where  $\beta_{BR}$  is the spectral energy slope defined by,  $f_v \propto v^\beta$  ( $f_v$  is the specific flux). This early evolution is unlikely to be related to the SN component. To date, color evolution has been observed in the light curves of GRB 021004, starting  $\sim 1.5$  d after the burst (Bersier et al. 2003; Mirabal et al. 2003), and possibly also in GRB 000301C (Rhoads & Fruchter 2001). An interpretation of the color change of GRB030329 in the context of the relativistic synchrotron model, as a manifestation of the cooling break frequency going through the optical bands (e.g., Galama et al. 2003) is discussed below (see §4.1).

## 4. DISCUSSION

### 4.1. Early breaks

The relative proximity of GRB 030329 has prompted special attention by the astronomical community, and several works presenting analysis of various data sets have been published so far. Our superior compilation of optical data, as well as the privilege afforded by the availability of these earlier works, allow us to inspect some previous suggestions in light of the newly available data.

Early analysis of preliminary optical data revealed that the slope of the optical decline became steeper around day 0.5 – 0.6 (e.g. Garnavich, Stanek, & Berlind 2003; Burenin et al. 2003; Price et al. 2003b). The change in the power-law decline index from  $\sim 1$  to  $\sim 2$ , seen both in early optical data and in sparse X-ray observations reported by Tiengo et al. (2003), combined with the achromatic nature of the break (Burenin et al. 2003), seemed to support an interpretation of this steepening as a “jet break” - the manifestation of a conical geometry in the relativistic emitting material (e.g., Rhoads 1997).

Figures 3 and 9 show that this simple interpretation does not fit the well sampled light curves now available. A model pos-

<sup>14</sup> A tabulated version of the “standard profile” is available in our website, <http://wise-obs.tau.ac.il/GRB030329/>

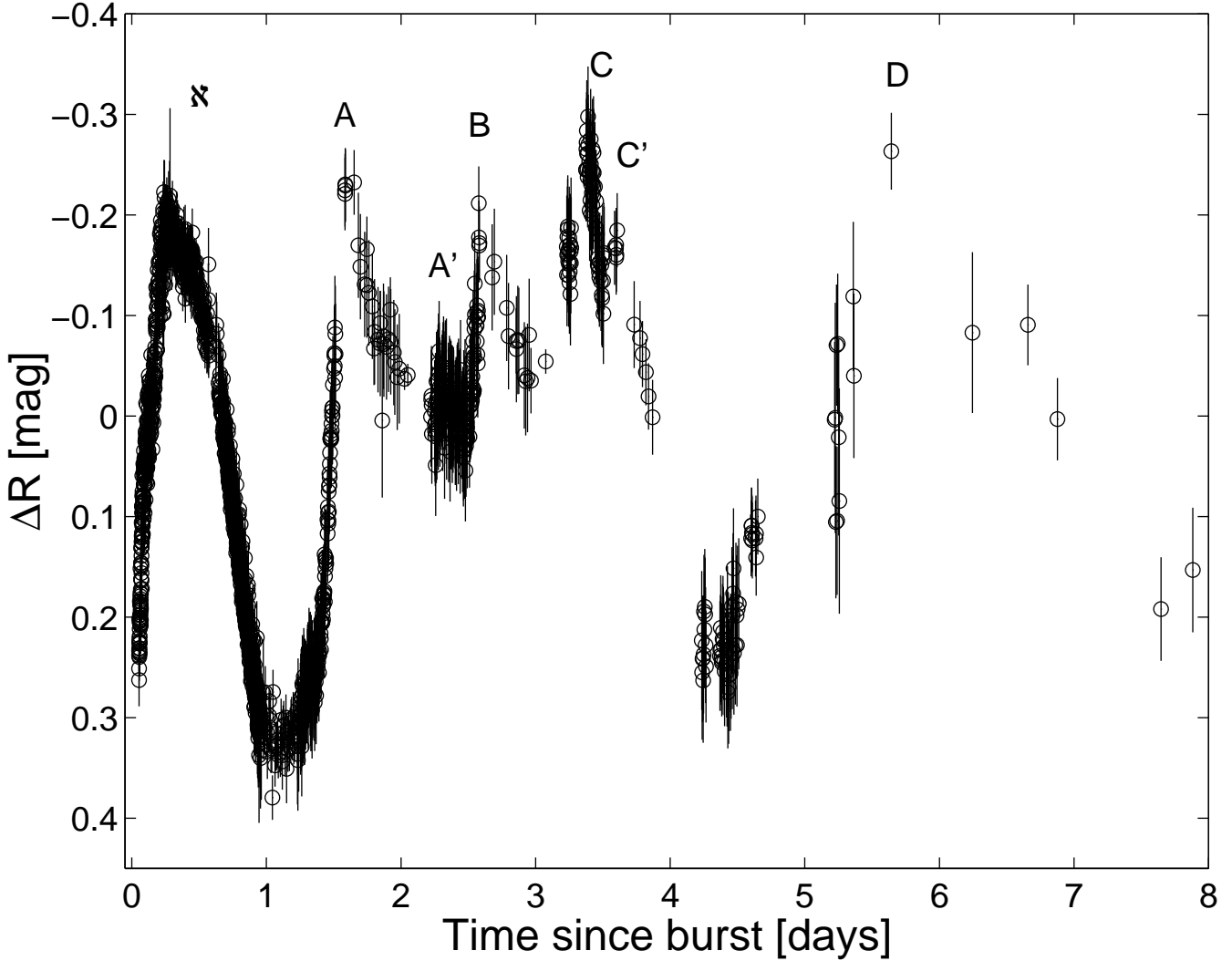


FIG. 4.— The residual light curve, obtained by subtracting our best fit double power-law (see text) from the light curve of the afterglow, during the first eight days after the burst. Five strong bumps, along with two possible minor ones, are apparent in the light curve.

tulating a steep ( $\alpha \sim 2$ ) optical decline starting at day  $\sim 0.5$  would severely under-predict the optical observations from day 1.5 onward. Sustaining a model involving a “jet break” at day 0.5 requires an additional source of optical emission emerging at day  $\sim 1$ . Such a model was indeed suggested by Granot et al. (2003) and Berger et al. (2003) and will be discussed in the next section.

As can be seen in Figures 4 and 9, as well as in Uemura et al. (2003) and Sato et al. (2003), the early optical data (i.e., before the suggested break at day  $\sim 0.5$ ) are not consistent with a single power-law decline, as predicted before a jet break. In particular, the data presented by Uemura et al. (2003), Torii et al. (2003), and Sato et al. (2003) require at least one additional break to occur around day  $\sim 0.25$ . Our compilation clearly elucidates this (Fig. 9). Several authors (Torii et al. 2003; Sato et al. 2003) suggested that this additional break (with a change in the temporal slope of  $\Delta\alpha \sim 0.3$ ) may represent the so-called “cooling break”, predicted in the context of relativistic fireball models (Sari, Piran & Narayan 1998) to occur as the cooling-break frequency,  $v_c$ , passes through the optical band (with  $\Delta\alpha = 0.25$ ). As seen in Fig. 9, the combination of an early cooling break at day 0.25 and a

jet break at day 0.5 allows a fair representation of the *early* optical data. Thus, successful models of this event should account for at least two early breaks. However, it should be stressed that the well sampled light curves available before 0.25 day are not consistent with a smooth power-law decline, and show significant wiggles and bumps (we shall further discuss this point below).

Previous studies suggesting an early cooling break relied on the analysis of single-band data, and could therefore only detect the predicted shift in the temporal decay slope  $\alpha$ , as discussed above. Our compilation also allows us to inspect the color evolution of the OT around the time of the suggested cooling break. As reported in §3.4, we detect a shift in the optical spectral index of  $\Delta\beta = 0.19 \pm 0.05$  between 0.28 (our earliest available color data) and 0.83 d after the burst.

Relativistic synchrotron models predict that a cooling break sweeping the optical band would manifest itself by a change in the color index of  $\Delta\beta = 0.5$ . If the observed color change is indeed due to the cooling break, then considering that  $\sim 40\%$  of the expected color change occurred between 0.28 to 0.83 days, and noting that both theory (Sari et al. 1998) and observations (Galama et al. 2003) show that the cooling break

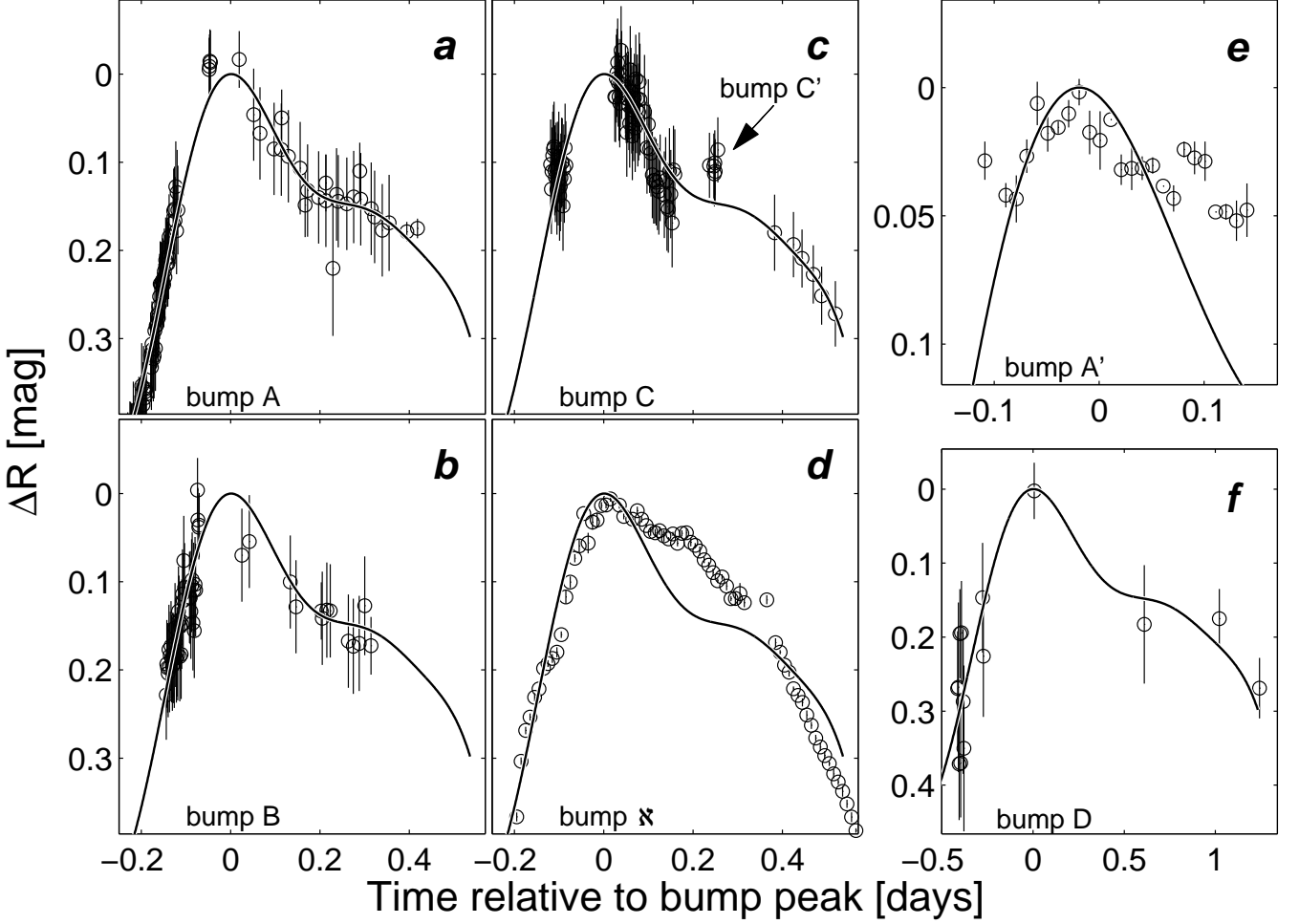


FIG. 5.— A close up view of the main bumps detected in the early residual light curve, which was obtained by subtracting our best fit double power-law (see text) from the light curve of the afterglow. Panels *a*, *b*, *c*, *d*, *e*, and *f*, display bumps *A*, *B*, *C*,  $\mathfrak{K}$ , *A'*, and *D*, respectively. The light curves in panels *d* and *e* were binned, to allow convenient browsing. The solid curves are a smoothed fit to the superimposed light curves of bumps *A*, *B*, and *C*, representing the common structure of these three bumps (see text for details). The time scale of the curve in panel *f* was stretched by a factor of 2.3.

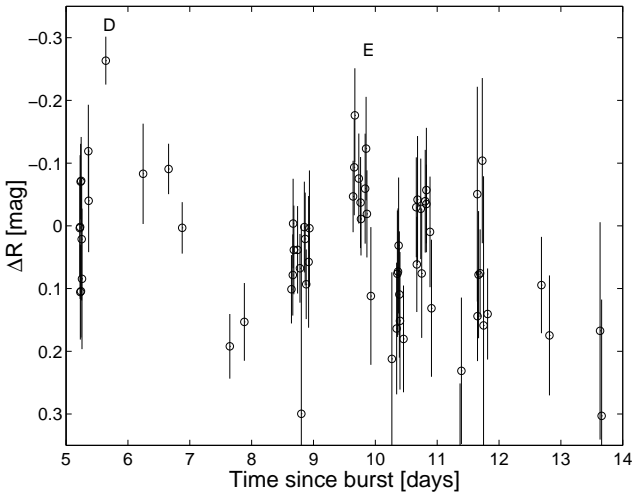


FIG. 6.— The variations light curve of the afterglow between day 5 and day 14.

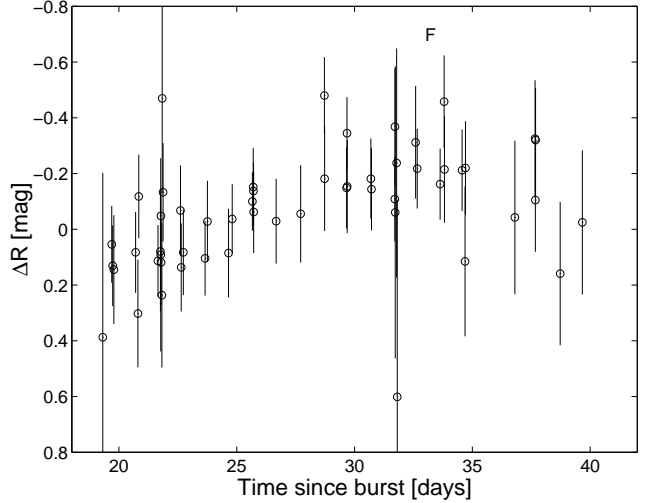


FIG. 7.— The variations light curve of the afterglow between day 18 day 42.

evolves in time with a power law, we estimate that the cooling

break crossed the  $V$  band at day  $\sim 0.25$ . We note that the

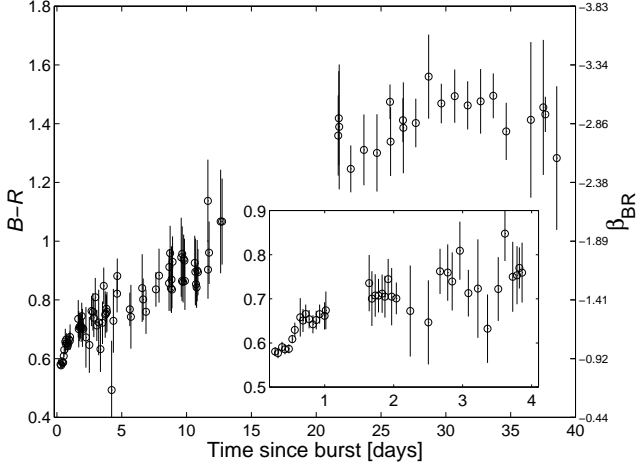


FIG. 8.— The binned ( $B-R$ ) color of the OT during the first 40 days after the burst. The vertical axis on the right shows the corresponding spectral power-law,  $\beta_{BR}$ . The inset is a blow-up of the first four days.

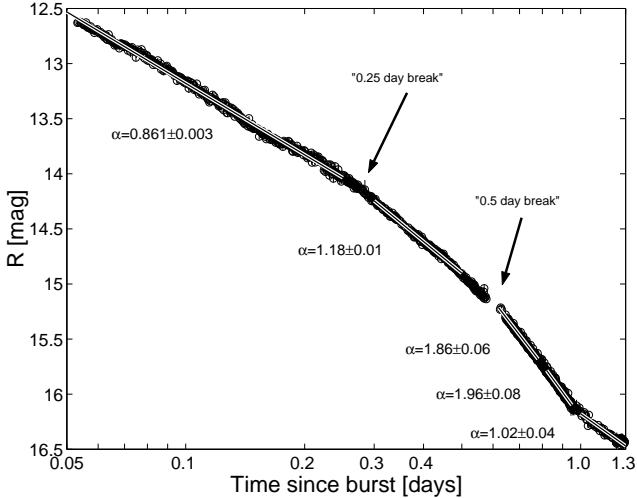


FIG. 9.— A detailed view of the early light curve of the OT associated with GRB 030329. The light curve distinctly breaks around 0.25 and 0.5 days. The data obtained prior to 0.25 days is not well described by a smooth power law, and shows significant wiggles. Note that our data rule out further steepening of the light curve at day 0.8, with the slope measured during 0.82–0.95 days consistent with the slope measured from earlier data (0.6–0.78 days) and certainly below the values  $\alpha \sim 2.2$  reported elsewhere (see text). Around day 1 the decline in the optical flux begins to slow, as the rising branch of bump A emerges.

observed steepening of the slope passed through the optical band from high frequencies to low ones, and hence demotes models predicting an opposite trend.

Another way to probe the cooling break frequency value during later times is through the optical to X-ray spectral index, which is predicted to be constant after the cooling break moves below the optical bands. We measured this in four epochs of XTE and XMM-Newton observations given by Tiengo et al. (2003;  $t = 0.222, 1.24, 37.24$ , and  $60.85$  d; the first epoch is the weighted mean of four measurements), by interpolating the  $R$ -band afterglow light curves onto the four epochs of the X-ray observations.

The value of slope at the first epoch  $-0.93 \pm 0.02$  (at  $t = 0.222$ ), before or during the proposed cooling transition, markedly differs from the values obtained at later epochs, after the break,  $-1.04 \pm 0.05$  and  $-1.06 \pm 0.13$  at  $37.24$  and

$60.85$  days after the burst, respectively. The value measured  $1.24$  days after the burst,  $-0.95 \pm 0.04$ , is consistent with both early and later values. A coherent picture therefore emerges from the optical observations and X-ray data in which the color evolution we detected is possibly the result of the cooling break passage through the optical band around  $0.25$  days after the burst. Naturally, other explanations for the observed early color evolution are possible.

Finally, we consider the report by Smith et al. (2003) of a further steepening of the optical light curve (reaching  $\alpha \sim 2.2$ ) around  $0.8$  day – distinct from, and occurring after the proposed  $0.5$  day break. This could have confirmed the prediction by Granot et al. (2003) that the final slope after a jet break around  $0.5$  days should be steeper than the value reported ( $\alpha = 1.9$ ), as expected from the temporal slope change due to a jet break,  $\Delta\alpha \sim 1$ , relative to the post-cooling break slope  $\alpha \sim 1.2$ . However, our superior data, including two mutually consistent data sets from the MDM and Mount Laguna Observatory, obtained through standard filters, are not consistent with the unfiltered data reported by Smith et al. (2003). Fig. 9 shows no segment of the early light curve (including the period between  $0.8$ – $1$  days) with a power-law slope steeper than  $\alpha = 2$ . Thus, the theoretically predicted slope of  $\alpha = 2.2$  was either not reached, or washed out by the emerging bump A.

To conclude, our results support the interpretation of the break around  $0.25$  days, as a cooling break, within the context of relativistic synchrotron models. The interpretation of later steepening of the light curve (around  $0.5$  day) as associated with a geometric (“jet”) break, can be sustained only if an additional emission source, dominating the optical flux from day  $1.5$  onward, is invoked.

It should also be noted that Dado, Dar, & De Rújula (2003) also put forward a theoretical prediction for the optical light curves of this event, based on their “cannon ball” model. Lacking access to the predicted curves, we are unable to conduct a detailed comparison with our data. However, such a comparison is certainly warranted, and could be easily conducted using our publicly available data.

#### 4.2. The two-jet model revisited

Berger et al. (2003) analyzed radio observations of GRB 030329, and found that the radio data, as well as mm-band observations reported by Sheth et al. (2003), could be well described by a relativistic jet model. However, the jet parameters indicated a “wide” jet, exhibiting the characteristic jet break about  $10$  days after the burst. In view of previous analysis of early-optical and X-ray data which seemed to require a “narrow” jet, breaking around day  $0.5$ , Berger et al. (2003) proposed a composite two-jet model, combining a narrow ultra-relativistic component responsible for the  $\gamma$ -rays and early ( $t \lesssim 1.5$  days) optical and X-ray afterglow, with a wide, mildly relativistic component responsible for the radio and optical afterglow beyond  $1.5$  days. This model provides a good fit to the radio and mm data as well as to the preliminary optical data used by these authors. The model also describes well the early X-ray observations, but under-estimates late ones. The wide jet component provides the additional source of emission required to account for the optical observations after day  $1.5$ , as discussed above.

The energy derived from the Frail relation (Frail et al 2001; Bloom et al. 2003), assuming only a narrow-jet component and the updated parameters used by Bloom et al. (2003), falls  $7\sigma$  below the geometrically corrected mean gamma-ray en-

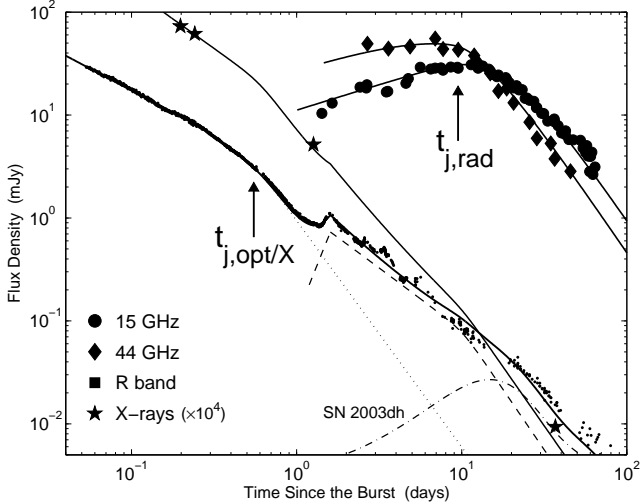


FIG. 10.— A comparison of the updated two-jet model with multi-band data. The model and notation are similar to those presented by Berger et al. (2003), except for several minor modifications (see text). The various symbols denote data points, as labeled, and the solid curves are the model predictions in each respective band. The model *R*-band light curve describes the general trends in the observed light curve well, but some discrepancies remain – the model becomes too bright around 10 days after the burst, and later on becomes two faint.

ergy of Bloom et al. (2003). The contribution of the wide-jet component introduced by Berger et al. (2003) brings the total energy to within  $1\sigma$  of the mean value of Bloom et al. (2003).

With our improved optical light curves at hand, we revisit the Berger two-jet model. Figure 10 shows a comparison between an updated two-jet model with radio data from Berger et al. (2003) and X-ray data from Tiengo et al. (2003), as well as our *R*-band light curve. The model is essentially the same as the one described in Berger et al. (2003), except for the following modifications. Firstly, a cooling break component at 0.25 day (see §4.1) was incorporated into the model. Additionally, the temporal emergence of the second jet at  $t \sim 1.5$  day was set to  $t^4$  (instead of the  $t^2$  law used in Berger et al. 2003) to account for the abrupt rise which our nearly continuous data show (in fact, an even steeper emergence is probably required). Finally, the 1998bw-based SN model used by Berger et al. (2003), which we showed to be too bright, was replaced by our best SN model as described in §3.1.

The modified two-jet model fairly describes the general trends in our well sampled optical light curves. However, some discrepancies still remain. Figure 11 shows the residuals obtained by subtracting the updated two-jet model from the observed *R*-band light curve. At early times ( $\lesssim 1.5$  day), the model fits the trends in the light curve. Nevertheless, significant undulations (with peak-to-peak  $\gtrsim 0.1$  mag), are detected about the smooth model (Fig. 12). Thus, this, or any other model based on broken power-law segments, should ultimately be supplemented with a mechanism explaining the bumpy nature of the optical emission, starting at the very earliest times (e.g., even prior to the cooling break). Following, a period of strong variations ensues, lasting till day eight. Comparing the inset in Figure 11 with Figure 4, we see that the two-jet model eliminates bump  $\aleph$  (which under this interpretation is the combined effects of the cooling and jet breaks) while bump  $A$ , associated with the emergence of the second jet, is diminished. However, later structure, including bumps

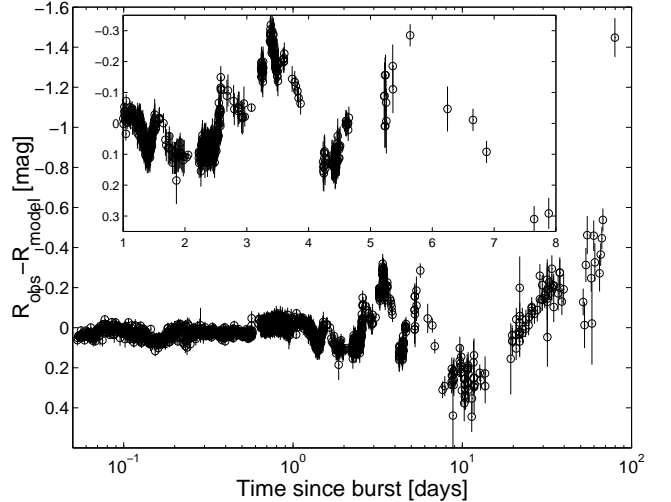


FIG. 11.— The residual light curve obtained by subtracting the modified two-jet model from the observed *R*-band light curve. Note that at  $t \leq 1$  day the model describes the general light curve trends very well, but significant wiggles around the smooth trend remain. A phase of strong variations can be seen between 1 – 8 days, followed by broader undulation around the predicted peak of SN 2003dh, that may be associated with inadequacies in the SN model. During later times ( $\gtrsim 20$  days), the data seem to require yet another source of optical emission, which is also strongly variable. The inset is a magnified view of the strong variations between, day 1 and day 8

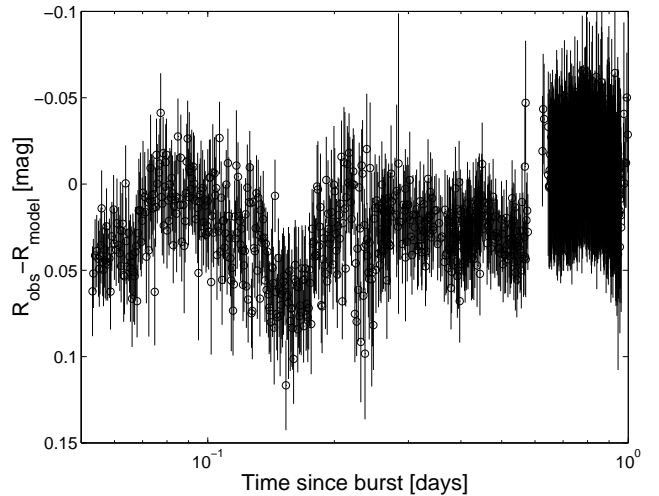


FIG. 12.— Same as Fig. 11, but zooming in on the period prior to the emergence of bump  $A$ . The residual undulations after subtraction of the Berger et al. (2003) two-jet model light curve are clearly evident.

$B$ ,  $C$ , and  $D$ , remains. Moreover, both the structure of these bumps and their peak-to-peak amplitude, are essentially unaltered. Thus, the modified two-jet model does not eliminate the need for an additional, strongly variable component of optical emission.

After day eight, a smooth undulation, lasting till day  $\sim 20$ , is seen in Figure 11. Since this is the period in which the optical flux is dominated by the emission from SN 2003dh, the discrepancy seen may indicate that our model light curve of SN 2003dh is at fault. This undulation can be almost completely removed by making our model for SN 2003dh fainter by 0.3 mag – at the lower limit of the range we consider plausible (see §3.1).

Finally, the data clearly require an additional source of op-

tical flux in order to explain the late-time ( $\gtrsim 20$  days) light curve. This extra component (in addition to the narrow and wide jets, and SN 2003dh) should *rise* from day 20 and through day 79, where our data end, and is also required to be strongly variable in order to explain the late time light curve “jitters”. This extra flux cannot be attributed to the SN without making its light curve very different from that of SN 1998bw, and highly variable. Further tests for the relative contribution of SN 2003dh to the late-time optical flux can be obtained from late-time spectroscopy of this event. Interestingly, as can be seen in the lower-right corner of Figure 10, the modified two-jet model also under-predicts the late-time X-ray points (at  $t = 37.24, 60.85$  day), perhaps indicating a need for an extra source of late-time flux in this band also.

To conclude, as already shown by Berger et al. (2003), the two-jet model provides a fair, self consistent description of observational data from the radio to the X-ray. However, in view of the large volume and complex nature of the multi-band data obtained for this event, further investigation of this model, perhaps combined with a prescription for the additional variations component required, is warranted.

#### 4.3. Can a single broken power-law provide a good fit to the data?

We demonstrated above that if we assume a power-law decline – the simplest OT model commonly used, the data require different slopes for the early- and late-time decline slopes (§ 3.2). The values of the decline indices,  $\alpha_1 \approx 1.1$  and  $\alpha_2 \approx 2$  are robustly constrained by the data. The transition between these decline slopes requires a break in the optical light curve  $\sim 3$  to  $\sim 8$  days after the burst. Unfortunately, the strong undulations superposed on the smooth decline trend throughout this period prevent us from determining the accurate timing of the power-law break.

It is intriguing to test whether this simple model, which naturally emerges from the analysis of the optical data, can consistently provide a reasonable fit to the entire multi-band data set gathered for this burst. In this context, we note the following major points. In the optical regime, this simple model for the “smooth” evolution of the OT requires additional emission component/components to account for the strong flux variability detected from hours to weeks after the burst. The ubiquity of these undulations suggests that such a component cannot be avoided by more complex models which have thus far been proposed. Particularly, as shown (§4.2), the two-jet model advocated by Berger et al. (2003) accounts for some of the more prominent features in the optical light curves of this event (X and A in Fig. 4), but does not account for other, equally prominent ones. Thus, without concrete and self-consistent models for the mechanism of the light curve variability, the amplitude of the undulations about the simple broken power-law model for this burst does not seem to argue against the validity of the single break model.

The X-ray coverage of this burst is regrettably sparse. Comparing the available data reported by Tiengo et al. (2003) with our optical light curves, and assuming that the X-ray and optical flux are correlated, as found by Fox et al. (2003) for GRB 021004, we expect the optical to X-ray slope index to remain approximately constant. As we have shown in §4.1, this is indeed the case, especially if the early X-ray point, obtained before the proposed cooling transition, is discarded. We note, however, that when over-plotting the X-ray data over the *R*-band light curve, and scaling the X-ray points to match the early light curve, the two latest XMM points fall below their

expected position, by a factor of 6–10. The physical significance of this discrepancy is not clear. We note, however, that a discrepancy of similar magnitude (but of opposite direction) is found also when comparing the modified two-jet model (§4.2) with the X-ray data (Fig. 10, bottom right corner). If any of these models is correct, this may suggest a weak evolution in the optical to X-ray spectral slope.

Finally, it appears that the greatest challenge for the simple one-break model is accounting for the results of the radio and mm observations. As elaborated by Berger et al. (2003), these data require the existence of a mildly-relativistic jet, which is expected to demonstrate a break in the optical regime around day 10 after the burst. Thus, the single break between  $\sim 3$  to  $\sim 8$  d after the burst implied by the simple model seems to be somewhat in odds with the constraints posed by the radio and mm data. However, no confidence intervals have been determined for the timing of the break, both in the optical and in radio. In the optical band, the measurement is hindered by strong, multiple bumps and wiggles superposed on the smooth light curves. The apparent conflict in the determination of the break time may perhaps be negotiated by future analysis, which would also model the variations in the optical band (e.g., by fitting a physically motivated model explaining the observed optical light curves). We thus conclude that the data at hand cannot rule out the empirically motivated singly-broken power-law model for the emission associated with GRB 030329. Assuming this model with  $t_{break} \approx 8$  day,  $E_{iso}(\gamma)$  as found in §4.2, and an interstellar matter density  $n = 1.8 \text{ cm}^{-3}$  (Berger et al. 2003), the estimated total energy of the event, derived using the Frail relation (Frail et al. 2001; Bloom et al. 2003), is  $4.4 \times 10^{50}$  erg. This value is within  $1.5\sigma$  of the updated geometrically corrected mean gamma-ray energy value of Bloom et al. (2003).

#### 4.4. Light Curve Variations

As shown above, the optical light curves of the OT associated with GRB 030329 exhibit strong undulations superposed on the overall smooth trends, detectable shortly (hours) after the burst, and still apparent many tens of days later. The variations seen during the period which is best-sampled by our light curves have a typical time scale of  $\sim 1$  day, and show a similar asymmetric structure, with a rising branch about twice as steep as the declining one. Both the characteristic amplitude ( $\sim 50\%$ ), and the structure of these variations are only weakly influenced by our assumptions about the underlying smooth behavior. In particular, similar results are obtained when we assume either the simple, empirically motivated, singly broken power-law model, or the more complex two-jet model of Berger et al. (2003; Figures 4 and 11, see inset).

Similar undulations have been previously observed in the light curves of OTs associated with GRBs. A short-time variation was detected in the light curves of GRB 000301C (e.g., Masetti et al. 2000; Rhoads & Fruchter 2001; Berger et al. 2000; Sagar et al. 2000). The short time scale and achromatic nature of the variation led Garnavich, Loeb, & Stanek (2000) to suggest this bump was caused by microlensing of the OT by a star in a foreground galaxy, while a more mundane origin for the bump – nonuniform ambient density – was proposed by Berger et al. (2000). The time scale and structure (fast rise, slow decline) of the bump detected in GRB 000301C, are similar to those seen in our light curves of GRB 030329. This, combined with the different structure seen in optical and IR light curves of the OT of GRB 000301C (Sagar et al. 2000), which also leads to a poor fit of the multi-band microlens-

ing model to the observed *R*-band light curve (Garnavich et al. 2000) suggests that the bump seen in the light curve of GRB 000301C is more likely to be intrinsic to the source, than the result of the rare cosmic alignment required for microlensing. More recently, numerous bumps were detected in the light curve of the OT associated with GRB 021004 (e.g., Bersier et al. 2003; Mirabal et al. 2003; Fox et al. 2003). Here too, the temporal structure and time scale of the bumps is similar to those seen in our light curves of GRB 030329.

A seemingly exceptional case to note is that of GRB 970508, the second burst for which an OT was identified. The optical transient of this burst (e.g., Galama et al. 1998) showed a major rebrightening around one day after the burst. Following a short rise lasting less than a day, the optical emission underwent a smooth, power-law decline over  $\sim 100$  days. The relatively sparse sampling of the light curve of this burst after day 10 does not allow us to determine the exact nature of the light curve decline during late phases (e.g., search for late “jitter” periods), but the overall smooth structure and very large amplitude of this rebrightening appear to be quite different from those of the OT associated with GRB 030329 (or from any other OT so far detected).

The common explanations for the short time-scale variations invoke complex density structures around the burst (e.g. Wang & Loeb 2000; Berger et al. 2000; Lazzati et al. 2002), inhomogeneous energy disposition within relativistic conical blast waves (the “patchy shell” model; Kumar & Piran 2000a) and continued injection of energy by the central engine (refreshed shocks; e.g., Rees & Mészáros 1998; Kumar & Piran 2000b). Nakar, Piran & Granot (2003) performed a detailed theoretical investigation of GRB 021004, and showed that variants of all these models can fit the data, although they preferred a version of the “Patchy Shell” model.

Granot et al. (2003) next studied the variability of GRB 030329, using a preliminary compilation of early optical data. Interpreting our detailed light curves in view of their analysis, we note the following points. The significant variations observed in the light curve before the proposed cooling break at day 0.25 probably argue against variable density models, in agreement with the conclusions of these authors. Interpreting the 0.5 day steepening in the light curve as a jet break, Granot et al. (2003) ruled out the patchy shell model, since it cannot produce strong variations after the entire jet is visible (i.e., after the jet break). Since strong variations are observed also well after day 10 (e.g., the “jitter episode”), the patchy shell model cannot explain the late variations observed in the light curve of GRB 030329. However, if the jet-break occurred as late as day eight (e.g., as in the single power-law model), the patchy shell model may explain the strong early variations.

The refreshed shocks scenario (Kumar & Piran 2002b), predicts that if the shocks occurred before the jet spreading, the time scale of the variations would be  $\Delta t \sim t$ . Granot et al. (2003) showed, however, that if the refreshed shocks occurred after the jet spreading, the time scale of the variations would be  $\Delta t \sim t^{1/4}$ . Considering the roughly constant time scale of the variations, and assuming a jet-break at day 0.5, Granot et al. (2003) favored the refreshed shocks model for the variations in the light curves of this burst. However, if a jet-break occurred after day  $\sim$ five, the almost constant time scale of the variations would be in contrast with the refreshed shocks model advocated by Granot et al. (2003). Inverting this argument, if refreshed shocks are shown to be the likely mech-

anism causing the observed variations, a model with a single jet break around day five becomes unphysical.

The similar structure of the undulations seen in the light curve of GRB 021004 (Nakar et al. 2003), GRB 000301C (Panaiteescu et al. 2001) and GRB030329, may hint on a “standard” variability mechanism in OTs. Naturally, many more cases should be studied in order to confirm this suggestion.

## 5. SUMMARY

We observed the optical afterglow of the nearby GRB 030329 from five observatories across the globe. We carefully cross-calibrated the observations, and augmented them with published data. The final compilation of *BVRI* light curves is unprecedented in its temporal sampling, and reveals complex structure.

Decomposing the light curve into host galaxy, SN, and afterglow components, we showed that SN 2003dh, associated with GRB 030329, could not have had a light curve identical to that of SN 1998bw. Instead, the evolution of SN 2003dh is better described by making the light curve of SN 1998bw fainter by 0.3 mag, and with a time scale that is 0.8 times shorter. We subtracted this SN model from the light curve of GRB 030329, and found that the residual light curve is well described by a double power-law, with a break point in the range of  $\sim 3$  to  $\sim 8$  days. The power-law slope of the light curve changed from  $\alpha_1 \approx 1.1$  to  $\alpha_2 \approx 2.0$ . These results are very weakly dependent on the SN model used.

The SN, host-galaxy, and power-law subtracted light curves of GRB 030329 show strong variations with time scales ranging from  $\sim 0.5$  hr to  $\sim 10$  d. The early variations ( $\lesssim 8$  days) which are well covered by our observations, are typically asymmetric with their ascending branch about twice as fast as the descending branch. Their typical, peak-to-peak time scales are 12 – 24 hr. Three of the bumps (A, B, and C) are of a similar structure during  $\sim 0.6$  days about their maximum. Later variations are harder to characterize, because of the lower frequency of our sampling. Nonetheless, they seem to have a longer time scale. Periods of strong variability are still evident in the light curve tens of days after the burst.

We showed that the OT color changed during the first day after the burst. In the context of relativistic synchrotron models, this supports the suggestions, based on single-band light curves, that the “cooling break” frequency passed through the optical bands around 0.25 days.

We discussed previous analysis of this event and found that the simple model involving a “jet break” occurring around day 0.5, proposed by several authors, is unable to account for the detailed optical data available for this event. At least two additional emission sources are required in order to sustain this interpretation: one to account for the flux observed from day one onward, as done by Berger et al. (2003), and another mechanism must be invoked to account for the ubiquitous undulations detected in the light curves throughout the observed period, i.e., both before and after the jet break.

Examining an updated version of the Berger et al. (2003) model, we find that it provides a fair description of available multi-band data. However, several discrepancies still need to be accounted for, probably requiring a self consistent model for the mechanism producing the ubiquitous bumps and wiggles in the light curves of this event. A similar effort is required in order to test a simpler, empirically-motivated singly-broken power-law model we present.

A comprehensive effort to model the large volume of data collected for this burst, explicitly accounting for the

variability on all time scales, appears like the next challenge in making this unique event a key to understanding the GRB phenomenon. In this vein, in order to ensure the maximal usefulness of our observations to the community, we make all the data available through our web site: <http://wise-obs.tau.ac.il/GRB030329/>.

We thank, M. Uemura and R.A. Burenin for sending us a digital version of their light curves, and the authors of the paper by Matheson et al. (2003) for the early release of their data to the community. We are grateful to A. Fruchter for sending us the host galaxy magnitude prior to publication. We ac-

knowledge fruitful discussions with E. Waxman, D. Frail, and A. Levinson. YML and EOO are grateful to the Dan-David prize foundation for financial support. AG acknowledges a Colton Fellowship. YML, EOO, AG, and DP  $\times 2$  were supported in part by grants from the Israel Science Foundation. We thank A. Henden and the USNO staff for providing us, and the GRB community in general, with field photometric calibration. We thank Eve Armstrong for observations at MDM, as well as the observers and staff of all the observatories who participated in this campaign, without which this work would not have been possible.

#### REFERENCES

Berezhiani, Z., Bombaci, I., Drago, A., Frontera, F., & Lavagno, A. 2003, *ApJ*, 586, 1250  
 Berger, E. et al. 2000, *ApJ*, 545, 56  
 Berger, E. et al. 2003, *Nature*, 426, 154  
 Bloom, J. S., Djorgovski, S. G., Kulkarni, S. R., & Frail, D. A. 1998, *ApJ*, 507, L25  
 Bloom, J. S. et al. 1999, *Nature*, 401, 453  
 Bloom, J. S. et al. 2002, *ApJ*, 572, L45  
 Bloom, J. S., et al. 2003, *AJ*, in press, as tro-ph/0308034  
 Bersier, D. et al. 2003, *ApJ*, 584, L43  
 Burenin, R. A. et al. 2003, *Astronomy Letters*, 29, 573  
 Castro-Tirado, A. J. et al. 1999, *Science*, 283, 2069  
 Chornock, R., Foley, R. J., Filippenko, A. V., Papenкова, M., Weisz, D., & Garnavich, P. 2003, *IAU Circ.*, 8114, 2  
 Dado, S., Dar, A., & De Rújula, A. 2003, *ApJ*, 594, L89  
 Esin, A. A. & Blandford, R. 2000, *ApJ*, 534, L151  
 Foley, R. J. et al. 2003, *PASP*, 115, 1220  
 Fox, D. W. et al. 2003, *Nature*, 422, 284  
 Frail, D. A. et al. 2001, *ApJL*, 562, L55  
 Galama, T. et al. 1997, *Nature*, 387, 479  
 Galama, T. J. et al. 1998a, *Nature*, 395, 670  
 Galama, T. J. et al. 1998b, *ApJ*, 497, L13  
 Galama, T. J., Frail, D. A., Sari, R., Berger, E., Taylor, G. B., & Kulkarni, S. R. 2003, *ApJ*, 585, 899  
 Gal-Yam, A., Ofek, E. O., & Shemmer, O. 2002, *MNRAS*, 332, L73  
 Garnavich, P. M., Loeb, A., & Stanek, K. Z. 2000, *ApJ*, 544, L11  
 Garnavich, P., Stanek, K. Z., Berlind, P., 2003, *GRB Circular Network*, 2018, 1  
 Garnavich, P. M. et al. 2003, *ApJ*, 582, 924  
 Granot, J., Nakar, E., & Piran, T. 2003, *Nature*, 426, 138  
 Greiner, J., Peimbert, M., Estaban, C., Kaufer, A., Jaunsen, A., Smoke, J., Klose, S., & Reimer, O. 2003a, *GRB Circular Network*, 2020, 1  
 Greiner, J. et al. 2003b, *Nature*, 426, 157  
 Harrison, F. A. et al. 1999, *ApJ*, 523, L121  
 Henden, A. 2003, *GRB Circular Network*, 2082, 1  
 Hjorth, J. et al. 2003, *Nature*, 423, 847  
 Kawabata, K. S. et al. 2003, *ApJ*, 593, L19  
 Kulkarni, S. R. et al. 1999, *Nature*, 398, 389  
 Kumar, P. & Piran, T. 2000a, *ApJ*, 535, 152  
 Kumar, P. & Piran, T. 2000b, *ApJ*, 532, 286  
 Lazzati, D., Rossi, E., Covino, S., Ghisellini, G., & Malesani, D. 2002, *A&A*, 396, L5  
 Masetti, N. et al. 2000, *A&A*, 359, L23  
 Matheson, T. et al. 2003, *ApJ*, 582, L5  
 Mazzali, P. A. et al. 2003, *ApJ*, 599, L95  
 McKenzie, E. H. & Schaefer, B. E. 1999, *PASP*, 111, 964  
 Mirabal, N. et al. 2003, *ApJ*, 595, 935  
 Nakar, E., Piran, T., & Granot, J. 2003, *New Astronomy*, 8, 495  
 Ofek, E. O. & Maoz, D. 2003, *ApJ*, 594, 101  
 Panaitescu, A. 2001, *ApJ*, 556, 1002  
 Panaitescu, A., Mészáros, P., & Rees, M. J. 1998, *ApJ*, 503, 314  
 Pandey, S. B., Anupama, G. C., Sagar, R., Bhattacharya, D., Sahu, D. K., & Pandey, J. C. 2003, *MNRAS*, 340, 375  
 Patat, F. et al. 2001, *ApJ*, 555, 900  
 Perlmutter, S. et al. 1999, *ApJ*, 517, 565  
 Peterson, B. A. & Price, P. A. 2003, *GRB Circular Network*, 1985, 1  
 Poznanski, D., Gal-Yam, A., Maoz, D., Filippenko, A. V., Leonard, D. C., & Matheson, T. 2002, *PASP*, 114, 833  
 Price, P. A. et al. 2001, *ApJ*, 549, L7  
 Price, P. A. et al. 2003a, *ApJ*, 589, 838  
 Price, P. A. et al. 2003b, *Nature*, 423, 844  
 Rees, M. J. & Mészáros, P. 1998, *ApJ*, 496, L1  
 Reichart, D. E. 2001, *ApJ*, 554, 643  
 Rhoads, J. E. 1997, *ApJ*, 487, L1  
 Rhoads, J. E. & Fruchter, A. S. 2001, *ApJ*, 546, 117  
 Sagar, R., Mohan, V., Pandey, S. B., Pandey, A. K., Stalin, C. S., & Castro-Tirado, A. J. 2000, *Bulletin of the Astronomical Society of India*, 28, 499  
 Sari, R., Piran, T., & Narayan, R. 1998, *ApJ*, 497, L17  
 Sari, R., Piran, T., & Halpern, J. P. 1999, *ApJ*, 519, L17  
 Sato, R., et al. 2003, *ApJ*, 599, L9  
 Schlegel, D. J., Finkbeiner, D. P. and Davis, M. 1998, *ApJ*, 500, 525  
 Sheth, K., Frail, D. A., White, S., Das, M., Bertoldi, F., Walter, F., Kulkarni, S. R., & Berger, E. 2003, *ApJ*, 595, L33  
 Smith, D. A. et al. 2003, *ApJ*, 596, L151  
 Sokolov, V. V., Kopylov, A. I., Zharikov, S. V., Feroci, M., Nicastro, L., & Palazzi, E. 1998, *A&A*, 334, 117  
 Stanek, K. Z., Garnavich, P. M., Kaluzny, J., Pych, W., & Thompson, I. 1999, *ApJ*, 522, L39  
 Stanek, K. Z. et al. 2003, *ApJ*, 591, L17  
 Stritzinger, M. et al. 2002, *AJ*, 124, 2100  
 Tiengo, A., Mereghetti, S., Ghisellini, G., Rossi, E., Ghirlanda, G., & ScharTEL, N. 2003, *A&A*, 409, 983  
 Torii, K. 2003, *GRB Circular Network*, 1986, 1  
 Torii, K. et al. 2003, *ApJ*, 597, L101  
 Uemura, M. et al. 2003, *Nature*, 423, 843  
 Urata, Y. et al. 2003, *ApJ*, accepted, astro-ph/0312145  
 van Paradijs, J. et al. 1997, *Nature*, 386, 686  
 Vanderspek, R. et al. 2003, *GRB Circular Network*, 1997, 1  
 Vietri, M. & Stella, L. 1998, *ApJ*, 507, L45  
 Wang, X. & Loeb, A. 2000, *ApJ*, 535, 788  
 Waxman, E. & Draine, B. T. 2000, *ApJ*, 537, 796  
 Yokoo, T., Arimoto, J., Matsumoto, K., Takahashi, A., & Sadakane, K. 1994, *PASJ*, 46, L191  
 Yoshii, Y. et al. 2003, *ApJ*, 592, 467  
 Zeh, A., Klose, S., & Hartmann, D. H. 2003, *ApJ*, submitted, astro-ph/0311610